Progress In Electromagnetics Research C, Vol. 57, 13–24, 2015

Effects of Chaotic Perturbation on a Periodic Gunn Oscillator

Bishnu C. Sarkar[1, *], Suvra Sarkar[2], Arun K. Guin[1], and Chaitali Koley[1]

Abstract—We have studied dynamics of a periodic X-band Gunn oscillator (GO) forced by microwave chaotic signals through numerical simulation and by hardware experiment. The chaos used as forcing signal is generated in a periodically driven non-oscillatory GO. Numerical simulation results indicate that the forced periodic GO becomes chaotic for a moderate strength of forcing chaos. The generated chaos in driven GO is found to become phase or general synchronized to the forcing chaos depending on strength of the latter one. Hardware experiments are performed in X-band of microwave frequency. It shows generation of chaos in driven GO due to forcing. Moreover, synchronization between forcing and generated chaos is indirectly verified.

1. INTRODUCTION

Dynamics of forced nonlinear oscillators has been studied over decades with different kinds of forcing signals [1–5]. The behaviour of forced oscillators primarily depends on relative strength and time domain nature of forcing signals. Several nonlinear responses like, synchronization, quasi periodicity and chaotic oscillations, are observed in the dynamics of forced oscillators [6, 7]. The quiescent operating condition of a driven system during forcing has important role in the ultimate state of dynamics. Several studies have reported asymmetric frequency locking, lock-in amplification, tracking noise filtering as well as synchronous angle demodulation properties of forced microwave oscillators [8–11]. In microwave frequency band, Gunn oscillators (GOs) are popular signal sources; they have low inherent noise and mechanical as well as electronic tuning facility [12, 13]. As such, nonlinear dynamics of forced GOs has drawn attention of the researchers [14–16]. Experimental studies presented in [17] have shown that building up and quenching phenomena of oscillation in a GO due to the variation of operating dc bias voltage show hysteresis. Also an under-biased GO (i.e., a GO biased below the threshold dc bias voltage required for normal oscillation) breaks into chaotic oscillation under the influence of an external periodic signal of appropriate frequency. The generation of microwave frequency chaos by this technique could be qualitatively proved with numerical simulation of mathematical model of the forced under biased GO. This technique of chaos generation is similar to parameter tuning technique of a forced non-oscillatory Rayleigh-Duffing oscillator [18, 19]. The onset of chaotic oscillations in different microwave oscillators has also been reported in the literature [20–24]. Further, in the condition of unilateral and bi-lateral coupling, two chaotic oscillators become synchronized. The required conditions for synchronization are (i) the oscillators are of nearly same frequency band, (ii) coupling strength is strong and (iii) generators use similar type of nonlinear devices [25, 26].

However, effects of forcing a periodic microwave oscillator with microwave frequency chaos have not been reported much, if any, and experimental results on this problem could hardly be found. In the present paper, we report our observations on the effect of forcing chaotic signal on a periodic GO. Our study incorporates experimental results obtained at X-band of microwave frequency. We have established the possibility of inducing chaotic oscillations in a forced GO through numerical integration of system equations. Also, we qualitatively prove the occurrence of generalised and phase

Received 12 February 2015, Accepted 19 March 2015, Scheduled 9 April 2015

* Corresponding author: Bishnu Charan Sarkar (bcsarkar_phy@yahoo.co.in).

[1] Department of Physics, Burdwan University, India. [2] Electronics Department, Burdwan Raj College, India.

synchronization between the forcing and generated chaos. The experimental study has established the fact that chaos could be induced in a periodic GO by forcing with chaotic signal of comparable frequency. The experimental evidence of synchronization between these two chaos signals has also been indirectly examined. The study reported in the paper would be useful in designing lock-in chaos amplifiers, modulators and demodulators for coherent chaos based communication systems, etc..

The rest of the paper is organized in the following way. Mathematical model of chaotic GO has been formulated in Section 2. Also system equations describing a periodic GO forced by chaotic signals are given in this section. The approach adopted in numerical solution and the results obtained thereof have been described in Section 3. Section 4 gives an account of the experimental study. In Section 5, some concluding remarks regarding numerical and experimental studies are incorporated.

2. FORMULATION OF MATHEMATICAL MODEL

In this section we present system equations of chaotic and periodic GO connected in a master slave configuration. The coupling between these GOs is made in practice by using circulators and attenuators. In the mathematical model, we consider the coupling as a diffusive one [6]. In Subsection 2.1 we represent system equation of a chaotic GO (CGO) and the same for the coupled system is presented in the next Subsection 2.2.

2.1. System Equation of a Chaotic GO (CGO)

Circuit theoretic model of a free running GO is shown in Fig. 1(a) and its mathematical equation in normalized form can be written as [27],

$$\frac{d^2q}{d\tau^2} = aq - bq^3 + c\left(\frac{dq}{d\tau}\right) - d\left(\frac{dq}{d\tau}\right)^3 \tag{1}$$

Here, τ is normalized time given by $\omega_r t$ where ω_r is the resonant angular frequency of the cavity and q the instantaneous charge normalized to unit charge. Parameters a, b, c and d depend on wave guide cavity geometry and biasing conditions of the device. It is similar to the equation of a Rayleigh-Duffing (R-D) oscillator [18]. For sustained oscillatory solution of (1) numerical values of parameters a, b, c, d should be positive [27]. In present study, we design a chaotic GO by forcing an under biased GO with a weak external microwave signal of comparable frequency. The GO is kept in positive differential resistance zone by applying a dc bias voltage less than threshold value required for NDR region of operation. Mathematically, this is ensured by a negative value of parameter c in (1) for non-oscillatory state of GO. Forcing it by an external signal of amplitude and normalized frequency, q_s and Ω, respectively, one gets chaotic oscillations. Thus the equation of GO capable of producing chaotic oscillations is [17],

$$\frac{d^2q}{d\tau^2} = aq - bq^3 + c\left(\frac{dq}{d\tau}\right) - d\left(\frac{dq}{d\tau}\right)^3 + q_s\cos\Omega\tau \tag{2}$$

2.2. System Equation for a PGO Forced by a CGO

The block diagram of coupled GO system is shown in Fig. 1(b). The arrangement for forcing a PGO by a CGO is designed with the help of three port circulators since a GO is a one port system. The mathematical model of this system can be derived considering the physics of operation of a forced GO by an external signal [28]. We use suffices 1 and 2 for the state variable q and system parameters a, b, c and d in the equations of CGO and PGO respectively. Thus, we get two equations as written below.

For forcing CGO:

$$\frac{d^2q_1}{d\tau^2} = a_1q_1 - b_1q_1^3 + c_1\left(\frac{dq_1}{d\tau}\right) - d_1\left(\frac{dq_1}{d\tau}\right)^3 + q_s\cos\Omega\tau \tag{3}$$

and for forced PGO:

$$\frac{d^2q_2}{d\tau^2} = a_2q_2 - b_2q_2^3 + c_2\left(\frac{dq_2}{d\tau}\right) - d_2\left(\frac{dq_2}{d\tau}\right)^3 + k_f\left(\frac{dq_1}{d\tau} - \frac{dq_2}{d\tau}\right) \tag{4}$$

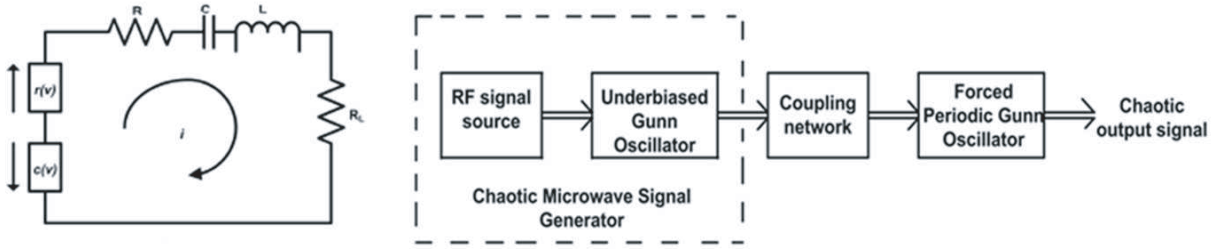

Figure 1. (a) A circuit theoretic equivalent representation of the Gunn oscillator used to formulate system Equation (1). The Gunn diode is represented by a series combination of voltage dependent resistor $r(v)$ and capacitor $c(v)$; R, C, L, R_L are lumped parameters equivalent to distributed circuit components of the wave guide type resonant cavity. (b) A functional block diagram of the system under study: a chaotic Gunn oscillator and a periodic Gunn oscillator are connected in a master-slave fashion.

k_f indicates the strength of coupling between CGO (master) and PGO (slave) systems. Values of parameters c_1 and c_2 are taken negative and positive quantities, respectively.

3. NUMERICAL SIMULATION AND RESULTS

We get the time domain dynamics of an isolated CGO by solving (2) with properly chosen GO and forcing signal parameters. As has been mentioned in Section 2.1, the value of parameter c is to be taken negative to ensure operation of the GO in under biased condition. We decompose (2) into two first order ODEs introducing a new state variable p, defined as the time derivative of q. Thus (2) is written as,

$$\frac{dq}{d\tau} = p \tag{5}$$

$$\frac{dp}{d\tau} = aq - bq^3 + cp - dp^3 + q_s \cos \Omega\tau \tag{6}$$

Here we substitute a new variable θ in place of $\Omega\tau$ in (6) and get a third ODE as,

$$\frac{d\theta}{d\tau} = \Omega \tag{7}$$

Time evolution of q and p are obtained by integrating (5), (6) and (7) using fourth order Runge-Kutta technique. Time increment steps are taken as 0.01 and initial values q_0 and p_0 are properly chosen. A sufficient number of solution points are discarded at the beginning of each simulation run, to obtain steady state dynamics of the system. Time domain variation of state variable q and phase plane diagram of $p - q$ are examined to understand the nature of oscillations of the GO. Moreover, frequency spectrum of q is obtained by taking fast Fourier transform (FFT) of the time series data. In numerical simulation, we take value of the parameter c negative (-0.002) to have below threshold operation (as noted in 2.1) and values of other parameters (a, b, d) are chosen from the knowledge of the dynamics of a GO reported in [22–24]. Note that a and b determine the oscillating frequency and d bounds the growth of sustained oscillation amplitude [22]. Among these parameters, c is most sensitive to bias voltage variation. So the tuning of value of c is taken in simulation study [17]. Values of Ω and q_s are taken equal to 1.27 and 0.15 for a set of simulation. This ensures the external forcing signal to be weak and of frequency equal to the resonant frequency of the cavity. In Figs. 2(a) and 2(b), the time development of q and its frequency domain representations are respectively given. It is evident from the figures that GO is oscillating in chaotic mode.

We derive Lyapunov exponent (LE) spectrum of forced GO described by (5)–(7) with the help of algorithm of Wolf et al. [29]. The system would have three LEs and a positive value of an LE would indicate chaotic oscillations. In Fig. 2(c) we depict the Lyapunov spectrum of the GO with c as a control

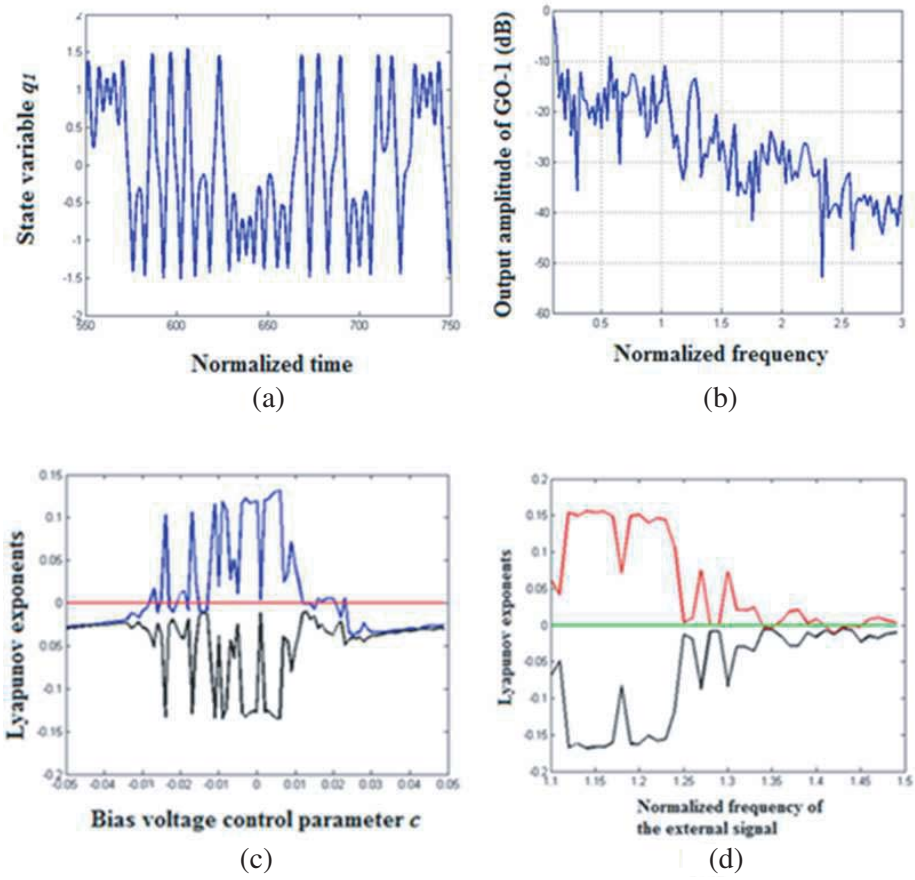

Figure 2. Numerical simulation results showing dynamics of a periodically driven under biased GO. (a) Time domain variation of the state variable q_1. (b) Frequency spectrum of the state variable q_1. (c) Lyapunov exponent spectrum with the bias voltage control parameter c. (d) Lyapunov exponent spectrum with the normalized frequency of the external driving signal [In Figs. 1(a) and 1(b) values of other system parameters taken are $a_1 = 1$, $b_1 = 1$, $c_1 = -0.002$, $d_1 = 0.015$, $q_s = 0.15$, $\Omega = 1.271$, in Fig. 1(c) parameter c and in Fig. 1(d) Ω are varied keeping other system parameters same as in Figs. 1(a) and 1(b) respectively].

parameter. Here we find that one of the LEs is positive when the value of c is around zero. This means that the chaotic oscillation of the GO occurs when the GO is biased close to the threshold bias ($c = 0$) and is driven by an external signal. However, when c is positive with a larger value, no LE is positive indicating non-chaotic oscillation. Fig. 2(d) depicts effect of variation of external signal frequency with negative value of c. Here we get one of the LEs positive for a particular range of Ω around the resonant frequency of the cavity. From these results we conclude that a driven under biased GO can be used as a microwave frequency chaos generator.

The dynamics of slave PGO forced by the output of the master CGO (henceforth mentioned as chaos-1) is obtained by solving the set of equations given in Section 2.2. Here, we would get a set of five ODEs, three for the non autonomous CGO having state variables q_1, p_1 and θ, while two ODEs for the driven PGO with state variables q_2 and p_2. The set of system equations is given as below.

$$\frac{dq_1}{d\tau} = p_1 \tag{8}$$

$$\frac{dp_1}{d\tau} = aq_1 - bq_1^3 + cp_1 - dp_1^3 + q_s \cos\theta \tag{9}$$

$$\frac{d\theta}{d\tau} = \Omega \tag{10}$$

$$\frac{dq_2}{d\tau} = p_2 \tag{11}$$

$$\frac{dp_2}{d\tau} = aq_2 - bq_2^3 + cp_2 - dp_2^3 + k_f(p_1 - p_2) \tag{12}$$

Numerical integration of the state equations is performed with the master GO in chaotic (c_1 is negative) and slave GO in periodic (c_2 is positive) mode. Variation of the value of parameter k_f is used to control the dynamics of forced PGO by chaos-1. The time series data of q_1 and q_2 are analysed to observe the state of forced PGO. LE spectrum of the coupled system with k_f as control parameter is shown in Fig. 3(a). It is observed that for a parameter set of CGO and PGO mentioned in the caption of Fig. 3, oscillations of driven PGO (slave system) becomes chaotic (henceforth mentioned as chaos-2) when k_f is more than 0.025. It is evident from a positive value of a second LE. The first positive LE is obtained due to chaos-1 from master GO.

Numerical simulations also indicate that chaos-1 and chaos-2 would become phase synchronized for

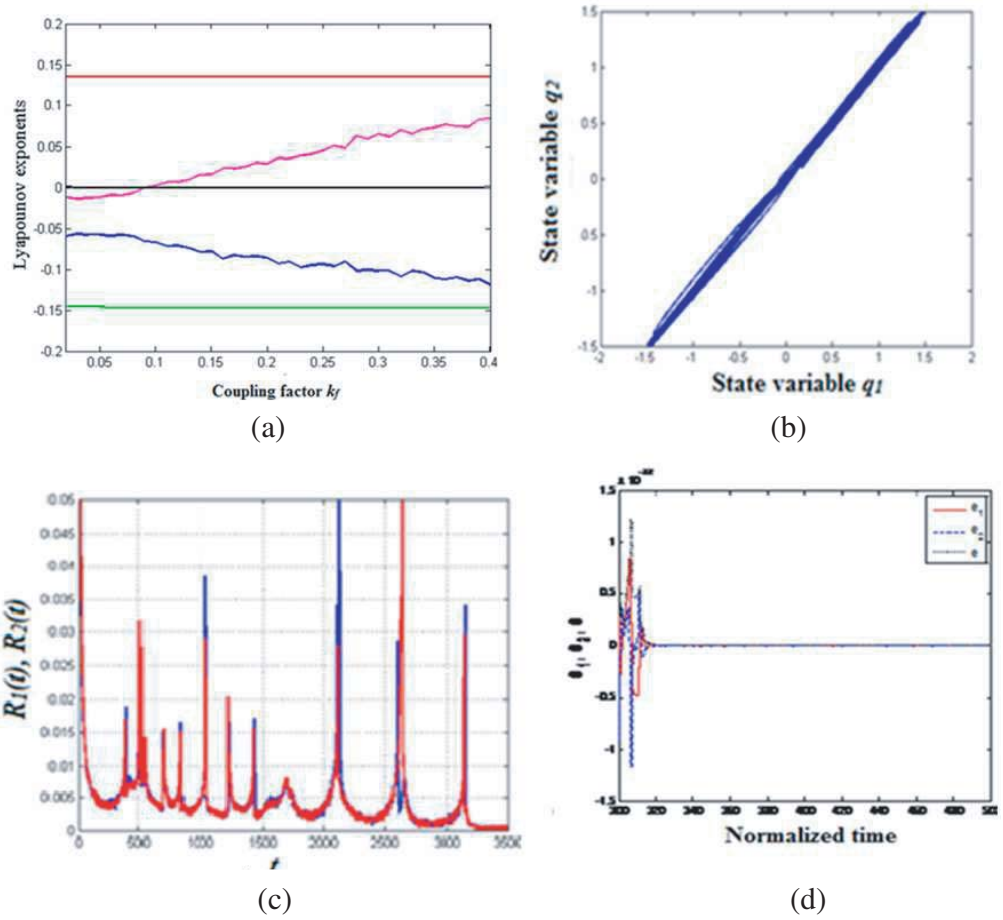

Figure 3. Numerically obtained results showing the dynamics of chaotic GO and periodic GO connected in master-slave configuration: (a) Lyapunov exponent spectrum with coupling factor (k_f) as control parameter. (b) State space trajectories ($q_1 - q_2$) for $k_f = 4.0$. (c) Generalized autocorrelation function (GAF) of the state variables q_1 and q_2 for $k_f = 4.0$. (d) Time variation of the error variables e_1, e_2 and e between the chaotically perturbed slave system and its auxiliary part for $k_f = 1.0$ [Values of other system parameters taken are $a_1 = a_2 = 1$, $b_1 = b_2 = 1$, $c_1 = -0.002$, $c_2 = 0.05$, $d_1 = d_2 = 0.015$, $q_s = 0.15$, $\Omega = 1.271$].

a range of values of k_f. We have plotted time series data of q_1 and corresponding q_2 along x-axis and y-axis respectively of Cartesian coordinate for different value of k_f. In case of phase synchronization, the plot of q_1-q_2 in Cartesian x-y coordinate system would be a straight line having 45° slope or an elliptic curve whose major axis is inclined at a fixed angle with the x-axis. Fig. 3(b) shows that chaos-2 is phase synchronized (PS) to chaos-1 for $k_f = 4.0$. But, they are not in PS condition for smaller values of k_f. Further, we can perform recurrence analysis on the time series data of q_1 and q_2 and estimate generalised auto-correlation function (GAF) and correlation of probability of recurrence (CPR). We write $R_1(t)$ and $R_2(t)$ as GAF of q_1 and q_2 respectively according to the definition given in [30, 31]. Plotting $R_1(t)$ and $R_2(t)$ on same graph and noting their coincidence we conclude regarding PS. Similarly for PS, CPR should be close to unity [30, 31]. Plots of generalized auto correlation function (GAF) of q_1 and q_2 are shown in same time scale in Fig. 3(c). The superposition of GAFs of q_1 and q_2 for $k_f = 4.0$ is observed. This is an indication of PS. We have also computed the CPR values for different k_f and find that these values become close to unity for larger value of k_f. For example, with k_f values 0.5, 1.0, 1.5 and 4.0 the computed CPR values are 0.9782, 0.9828, 0.9866 and 0.9912 respectively.

We examine the possibility of generalized synchronization (GS) between chaos-1 and chaos-2 by auxiliary system approach [32, 33]. In this approach, we consider two slave PGOs driven by the same chaotic signal obtained from the master CGO. All design parameters of the two slaves are identical, but they have different initial conditions. Two state variables for the first and the second slave systems are respectively taken as q_2, p_2, and q_2', p_2'. Thus state equations of the second slave would be given by (11) and (12), only, replacing q_2 with q_2' and p_2 with p_2'. Now we define two instantaneous error variables e_1 and e_2 as $(q_2 - q_2')$ and $(p_2 - p_2')$ respectively. After performing a bit of manipulation we obtain the time evolution equations for e_1 and e_2 as:

$$\frac{de_1}{d\tau} = e_2 \tag{13}$$

$$\frac{de_2}{d\tau} = a_2 e_1 - b_2 e_1^3 - 3b_2 e_1 q_2' q_2 + c_2 e_2 - d_2 e_2^3 - 3d_2 e_2 p_2 p_2' - k_f e_2 \tag{14}$$

The time development of e_1 and e_2 is numerically obtained by solving a set of nine first order ODEs, three for the master CGO as given in (8)–(10), four for two slave systems (two for each slave with different initial conditions as (11) and (12)) and two for error variables ((13) and (14)). If e_1 and e_2 tend to zero asymptotically, occurrence of GS is confirmed. Intuitively, average distance between the system trajectories of the two slave systems in phase space is $e = \sqrt{e_1^2 - e_2^2}$. In the condition of GS, two slaves would follow the master in identical manner and this will make the average distance between the trajectories zero asymptotically. Fig. 3(d) depicts time domain variation of e_1, e_2 and e for $k_f = 1.0$. It has been observed that for $k_f = 0.1$ the error variables do not converge to zero for increasing time. Thus there is no possibility of GS with such amount of coupling factor; but for $k_f = 1.0$, error variables converge to zero asymptotically in time and GS is ensured. We note that for PS we need larger value of k_f compared to those required for GS.

4. EXPERIMENTAL STUDY

We perform a hardware experiment to study the dynamics of a driven GO with chaotic signal of comparable frequency and to observe the state of synchronization between the driving and generated chaos (chaos-1 and chaos-2). But we cannot experimentally measure the state of synchronization in real time due to non-availability of time domain instrument in X band microwave frequency in our laboratory. So we adopt an alternative indirect proof of synchronization using a correlator-averager arrangement. Here we multiply two signals whose relative states are to be obtained and take time average of the product. In synchronized condition, we get a dc voltage as the averager output.

4.1. Experimental Arrangement

Figure 4 shows block diagram of experimental setup. Here, GO-1 generates forcing chaos signal (chaos-1) and GO-2 operates as the driven periodic oscillator. As such, GO-1 is operated in the under biased condition with an injected RF field into its cavity. This RF signal is taken from a microwave signal

source (MSS). Chaos-1 is taken out through circulator CR-1 and is power amplified using an X-band microwave power amplifier (MPA). An attenuator (ATN) is used to vary the strength of chaos-1 to be injected into GO-2 through circulator CR-2. The output of GO-2 (chaos-2) is taken out at port 3 of CR-2. To compare the state of oscillation of chaos-2 with respect to chaos-1, we use a phase comparator circuit (PCC) [34]. It is designed using a magic tee, two diode detectors, a difference amplifier (DA) and a low pass filter (LPF) as shown in Fig. 4. The output dc voltage of PCC is a measure of phase difference between two inputs applied to the PCC.

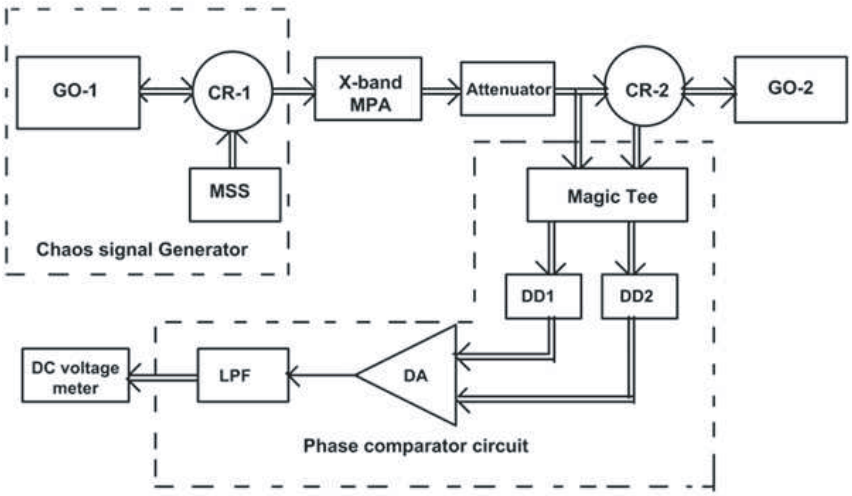

Figure 4. Block diagram of the experimental arrangement used in the study.

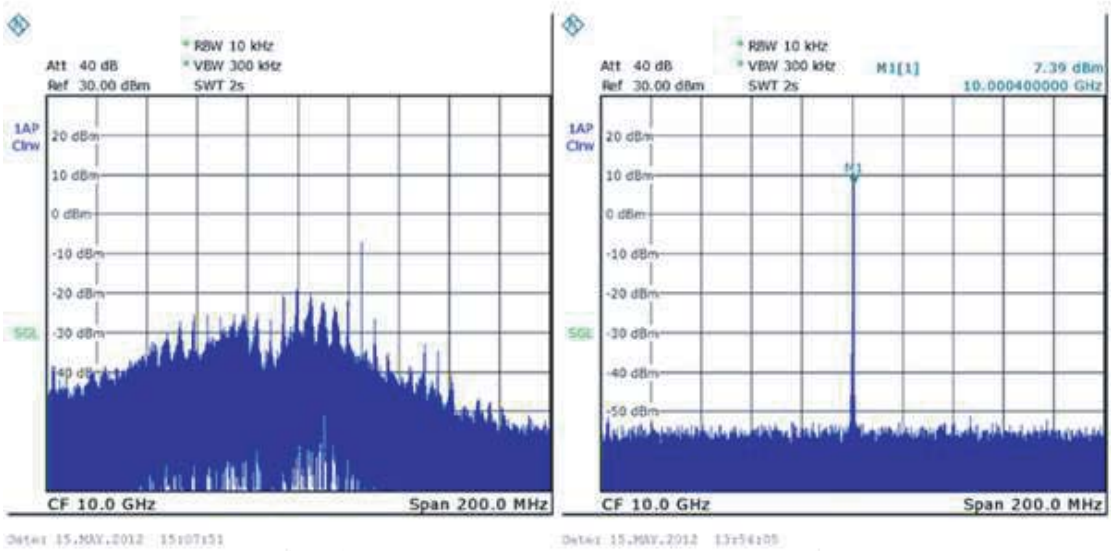

(a) (b)

Figure 5. Experimentally obtained output power frequency spectrum of master and slave GOs in isolated condition, (a) chaotic GO (operating dc bias voltage is 4.76 Volt and it is driven by an external RF signal of frequency 10.025 GHz and power 0 dBm, (b) periodic GO (operating dc bias voltage 9.20 Volt, frequency and output power of the generated periodic signal are 10 GHz and 11 dBm respectively).

4.2. Experimental Results

A properly biased GO would produce periodic signal. At operating dc bias voltage 9.2 volts, we adjust cavity dimension to get GO oscillation frequency 10 GHz. The output power is measured as 11 dBm and its spectrum is shown in Fig. 5(a). Adjusting dc bias at 4.62 volts (below the threshold voltage 6.2 volts required for oscillation) and applying an external signal of frequency 10.25 GHz and power 0 dBm, we obtain chaotic oscillations in the GO and it is shown in Fig. 5(b). It has a 20 dBm bandwidth of amount 100 MHz.

In coupled system, power of chaos-1 is varied using an attenuator shown in the experimental arrangement (Fig. 4). The output spectrum of the driven GO is shown in Figs. 6(a) to 6(d) for

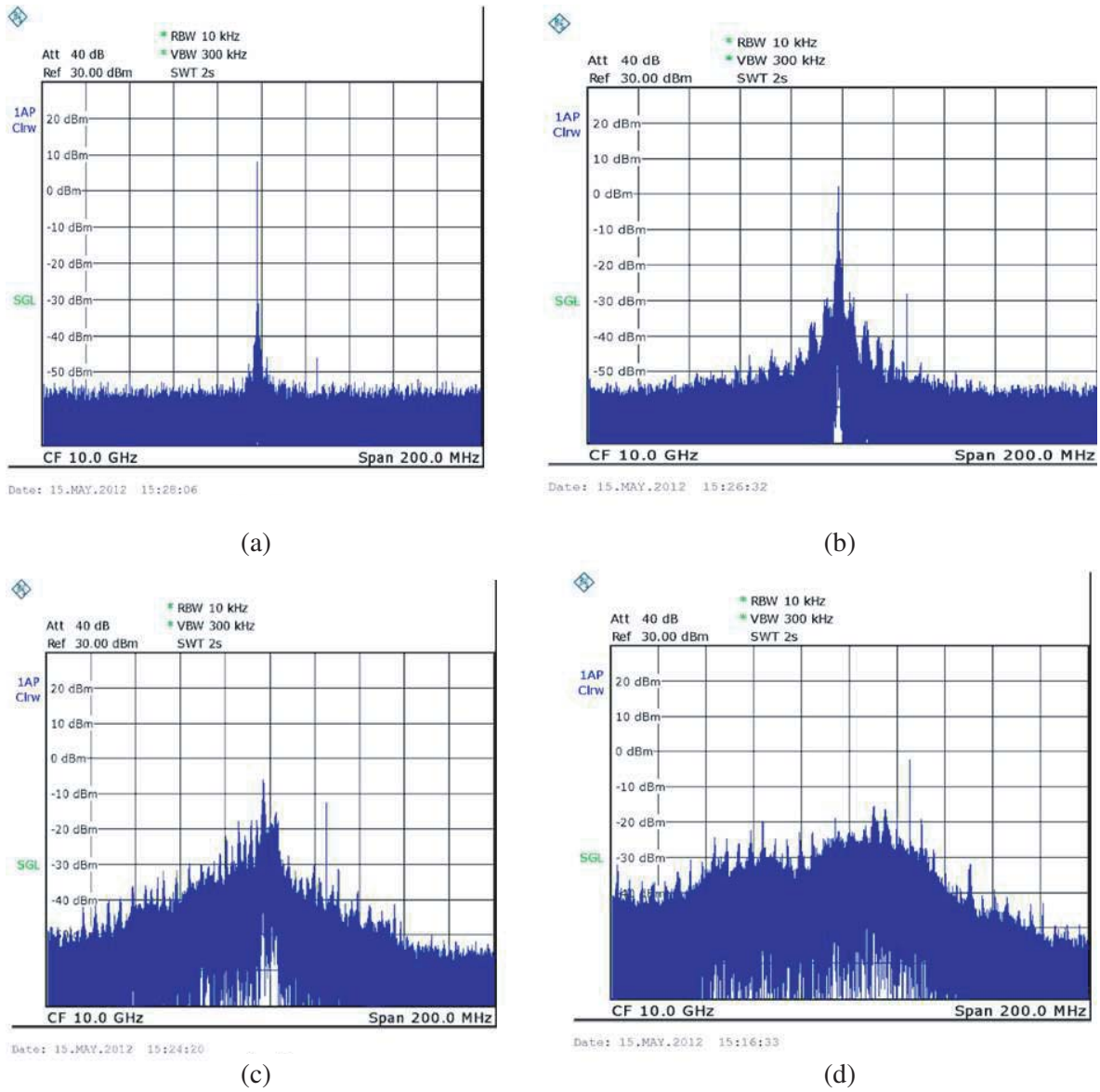

Figure 6. Experimentally obtained output power frequency spectrum of the driven GO for different strengths of the injected chaotic signal. The amounts of injected power are respectively, (a) 0.1%, (b) 0.9%, (c) 15% and (d) 57.8% of the output power of the forcing GO. Frequency and output power of the isolated driven PGO are 10 GHz and 11 dBm respectively.

different strengths of chaos-1. It shows that with the increase of strength of injected chaos, output spectrum of driven GO gradually changes from a line spectrum to a broad band spectrum. The broad band spectrum of driven GO output proves the generation of chaotic oscillations (chaos-2) and this is obtained for reasonably strong injected chaotic signal.

Finally, we adopt following indirect method to experimentally verify synchronization between chaos-1 and chaos-2. We find time average of the product of chaos-1 and chaos-2 and when this time average signal is a dc voltage (with small fluctuations), we infer the occurrence of synchronization between them. At first a reference observation is made studying the phenomenon of forced synchronization of a PGO to a sinusoidal forcing signal. The forcing signal is taken from a GO operating in normal

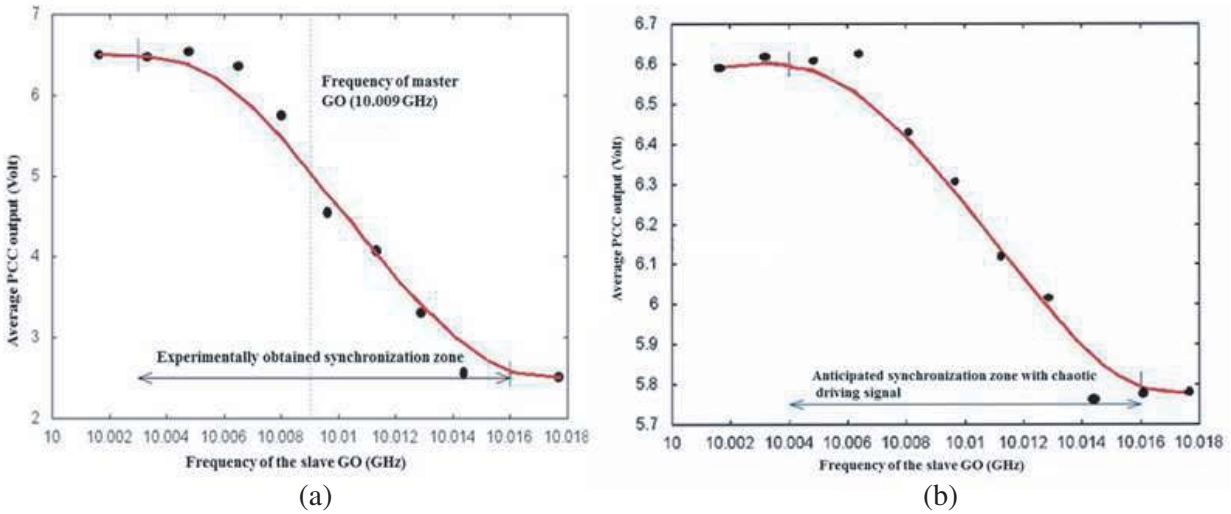

Figure 7. Experimentally obtained PCC output dc voltage vs frequency of the driven PGO (obtained by varying its wave guide dimension) curves. Forcing signal is (a) sinusoidal, (b) chaotic.

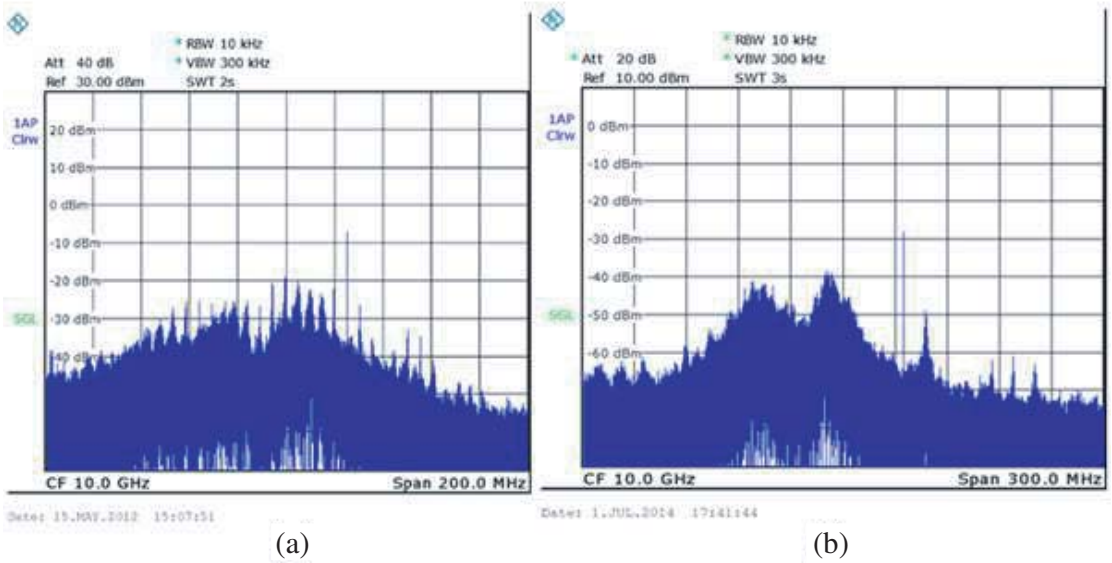

Figure 8. Experimentally obtained output power spectrum of: (a) driving chaos, (b) generated chaos in the anticipated synchronized condition of two chaotic oscillations.

condition. The frequency of driven PGO is changed by varying the length of GO cavity. Frequencies of two signals are directly measured using two spectrum analysers. Fig. 7(a) shows the variation of time averaged product at this condition. Here we get a zone of synchronization where master and slave GOs have *same frequencies*. In this zone of same frequency of two GO (indicated in Fig. 7(a)), the time average of PCC output is found to vary monotonically with frequency of driven GO. The presence of this range of monotonic dc voltage variation is *an indirect proof* of synchronization. Next we perform the same experiment with a chaotic injected signal. Frequency of slave PGO is varied in a similar way and we note a zone of monotonic variation of time averaged PCC output. Results obtained for this part of experiment are shown in Fig. 7(b). The nature of the curve shown in Fig. 7(b) has a qualitative similarity with that shown in Fig. 7(a) for a range of frequency. When the dc voltage varies monotonically, we conclude (*from indirect evidence*) that synchronization between chaos-1 and chaos-2 has taken place. We note that synchronization occurs when (i) power of injected chaos is at least 30% of power of driven GO, and (ii) frequency band of injected chaos is to be around the driven PGO frequency. Fig. 8 shows representative frequency spectrum of driving chaos and generated chaos within the anticipated synchronization zone.

5. CONCLUSION

The present paper reports results of our study regarding effects of chaotic perturbation on a periodic GO. The study has been carried out by numerical simulation of system equations and by hardware experiment. The findings of simulation study are as given below: (i) periodic GO becomes chaotic due to chaotic perturbation; (ii) generated chaos in driven GO becomes synchronized in general sense with moderately strong driving chaos; (iii) phase synchronization between these two chaotic signals occurs for increased power of driving chaos. In simulation study GS is established by well-known technique of auxiliary system approach. PS is proved by finding GAF and CPR from time series data of driving and driven chaos.

The paper incorporates results of our experimental studies performed using X-band GOs. The obtained experimental results confirm following observations of simulation study: (i) generation of microwave chaos is possible using under biased periodically driven GOs; (ii) a periodically oscillating GO becomes chaotic due to perturbation by chaotic signal; (iii) synchronization between forcing chaotic signal and generated chaos in a forced GO is experimentally examined through indirect method. Due to non-availability of time domain experimental results, comparison of simulation and experimental results could not be quantitatively made. Moreover, in the present work, we have not attempted to identify *route to chaos* in the dynamics of chaotically perturbed periodic GO.

ACKNOWLEDGMENT

Authors thankfully acknowledge the infrastructural support received from the DST (India) and the BRNS (DAE, India) through sponsored research projects in carrying out the work. They also acknowledge the support received from the DST, India through the PURSE program of the University of Burdwan, West Bengal, India.

REFERENCES

1. Adler, R., "A study of locking phenomena in oscillators," *Proceedings of the IEEE*, Vol. 61, 1380–1385, 1973.
2. Diakoku, K. and Y. Mizushima, "Properties of injection locking in the non-linear oscillator," *International Journal of Electronics*, Vol. 31, 279–292, 1971.
3. Jensen, R. V., "Synchronization of driven nonlinear oscillators," *American J. Physics*, Vol. 70, 607–619, 2002.
4. Rajavi, B., "A study of injection locking and pulling in oscillators," *IEEE Journal of Solid State Circuits*, Vol. 39, 1415–1424, 2004.

5. Li, C. J., C. H. Hsiao, F. K. Wang, T. S. Horng, and K. C. Peng, "A rigorous analysis of a phase locked oscillator under injection," *IEEE Transactions on Microwave Theory and Techniques*, Vol. 58, No. 5, 1391–1400, 2010.
6. Pikovsky, A., M. Rosenblum, and J. Kurth, *Synchronization: A Universal Concept in Nonlinear Sciences*, Cambridge University Press, Cambridge, 2003.
7. Stogartz, S. H., *Nonlinear Dynamics and Chaos: With Applications to Physics, Biology, Chemistry and Engineering*, Levant Books, Kolkata, India, (Indian Edition), 2007.
8. Kurokawa, K., "Injection locking of microwave solid state oscillator," *Proceedings of the IEEE*, Vol. 61, 1386–1410, 1973.
9. Alekseev, Y. I., "Determination of basic characteristics of synchronization of Gunn self-excited oscillators," *Instruments and Experimental Techniques*, Vol. 50, 241–243, 2007.
10. Main, E. and D. Coffing, "FM demodulation using an injection locked oscillator," *IEEE MTT-S International Microwave Symposium Digest*, Vol. 1, 135–138, 2000.
11. Ko, D. S., S. J. Lee, T. J. Baek, S. G. Choi, M. Han, H. C. Park, J. K. Rhee, J. H. Jung, and Y. W. Park, "New tuning method for 94 GHz waveguide voltage controlled oscillator," *IEEE Microwave and Wireless Components Letters*, Vol. 21, 2011.
12. Bates, R. S. and S. Feeney, "Novel varactor tuned millimeter wave Gunn oscillator," *Electronics Letters*, Vol. 23, 714–715, 1987.
13. Zhu, X., Y. Chen, and W. Hong, "Q-band injection-locked Gunn diode oscillator," *International Journal of Infrared and Millimeter Waves*, Vol. 17, No. 3, 527–533, 1996.
14. Mosekilde, E., et al., "Mode locking and spatio-temporal chaos in periodically driven Gunn diode," *Physical Review B*, Vol. 41, 2298–2306, 1990.
15. Zongfu, J. and M. Benkun, "Period doubling and chaos in the Gunn effect," *Physical Review B*, Vol. 44, 11072–4, 1991.
16. Chakraborty, J., T. Banerjee, R. Ghatak, A. Bose, and B. C. Sarkar, "Generating chaos in injection-synchronized Gunn oscillator: An experimental approach," *IETE Journal of Research*, Vol. 55, 106–111, 2009.
17. Sarkar, B. C., C. Koley, A. K. Guin, and S. Sarkar, "Some numerical and experimental observations on the growth of oscillations in an X-band Gunn oscillator," *Progress In Electromagnetics Research B*, Vol. 40, 325–341, 2012.
18. Siewe, M. S., H. Cao, and M. A. F. Sanjuan, "Effect of nonlinear dissipation on the basin boundaries of a driven two-well rayleigh-duffing oscillator," *Chaos, Solitons and Fractals*, Vol. 39, 1092–1099, 2009.
19. Musielak, D. E., Z. E. Musielak, and J. W. Banner, "Chaos and route to chaos in coupled duffing oscillators with multiple degree of freedom," *Chaos, Solitons and Fractals*, Vol. 24, No. 4, 907–922, 2005.
20. Jiang, T., S. Qiao, Z.-G. Shi, L. Peng, J. Huangfu, W.-Z. Cui, W. Ma, and L.-X. Ran, "Simulation and experimental evaluation of the radar signal performance of chaotic signals generated from a microwave Colpitts oscillator," *Progress In Electromagnetics Research*, Vol. 90, 15–30, 2009.
21. Shi, Z. G. and L. X. Ran, "Microwave chaotic Colpitts oscillator: Design, implementation and applications," *Journal of Electromagnetic Waves and Applications*, Vol. 20, No. 10, 1335–1349, 2006.
22. Sarkar, B. C., D. Sarkar, S. Sarkar, and J. Chakraborty, "Studies on the dynamics of bilaterally coupled X-band Gunn oscillators," *Progress In Electromagnetics Research B*, Vol. 32, 149–167, 2011.
23. Ram, R. J., R. Sporer, H. R. Blank, and R. A. York, "Chaotic dynamics in coupled microwave oscillators," *IEEE Transactions on Microwave Theory and Techniques*, Vol. 48, 1909–1916, 2000.
24. Chakravorty, J., S. Sarkar, and B. C. Sarkar, "Studies on the dynamics of driven bilaterally coupled Gunn oscillator," *Indian Journal of Science and Technology*, Vol. 7, 916–923, 2014.
25. Volos, C. K., I. M. Kyprianidis, and I. N. Stouboulos, "Experimental synchronization of two resistively coupled Duffing type circuits," *Nonlinear Phenomena in Complex Systems*, Vol. 11,

187–192, 2008.

26. Zhigang, Z., X. Wang, and M. C. Cross, "Transition from partial to complete generalized synchronization in bilaterally coupled chaotic oscillators," *Physical Review E*, Vol. 65, 056211, 2002.
27. Sarkar, B. C., "Nonlinear dynamics of Gunn oscillator," (Book chapter), *New Research Trends in Nonlinear Circuits: Design, Chaotic Phenomena and Applications*, Chapter 2, Nova Publishers, 2014.
28. Sarkar, B. C., S. Sarkar, C. Koley, A. K. Guin, and T. Banerjee, "Effects of unilateral coupling between two chaotic X-band Gunn oscillators," *International Journal of Bifurcation and Chaos*, Vol. 23, 1350185-1–23, 2013.
29. Wolf, A., J. B. Swift, H. Swinney, and J. A. Vastano, "Determining Lyapunov exponents from a time series," *Physica D*, Vol. 16, 285–317, 1985.
30. Romano, M. C., M. Theil, J. Kurths, Z. I. Kiss, and J. L. Hudson, "Detection of synchronization for non phase coherent and non stationary data," *Europhysics Letters*, Vol. 71, 462–472, 2005.
31. Marwan, N., M. Romano, M. Thiel, and J. Kurths, "Recurrence plots for the analysis of complex system," *Physics Reports*, Vol. 438, 237–329, 2007.
32. Rulkov, N. F., M. M. Sushchik, L. S. Tsimring, and H. D. I. Abarbanel, "Generalized synchronization of chaos in directionally coupled chaotic systems," *Physical Review E*, Vol. 51, 980–994, 1995.
33. Abarbanel, H. D. I., N. F. Rulkov, and M. M. Sushchik, "Generalized synchronization of chaos: The auxiliary system approach," *Physical Review E*, Vol. 53, 4528–4535, 1996.
34. Sarkar, S., T. Banerjee, D. Mondal, and B. C. Sarkar, "Theory and performance of an electrically controlled microwave phase shifter," *Indian Journal of Pure and Applied Physics*, Vol. 43, 215–220, 2005.